SLAC-PUB-9655
February 2003

Analysis of Statistical Correlations and Intensity Spiking in the Self-Amplified Spontaneous-Emission Free-Electron Laser*

S. Krinsky[1]
Stanford Linear Accelerator Center, Stanford, CA 94309
R.L. Gluckstern
Department of Physics, University of Maryland, College Park, MD 20742

Abstract

The narrow band chaotic output of the self-amplified spontaneous-emission free-electron laser (SASE FEL) exhibits intensity spikes. In the linear regime before saturation, we use an approach developed by Rice to determine probability distributions for the peak values of intensity in both the time and frequency domains. We also find the average number of spikes per unit time or frequency. In addition, we derive joint probabilities for the intensity in the output pulse to have values I_1 and I_2 at times t_1 and t_2, and for the spectral intensity to have values $\tilde{I}_1$ and $\tilde{I}_2$ at frequencies ω_1 and ω_2.

PACS: 41.60.Cr, 02.50.-r

Submitted to: Physical Review ST-AB

[1] Permanent address: Brookhaven National Laboratory, Upton, NY 11973

* Work supported by Department of Energy contracts DE–AC03–76SF00515 and DE-AC02-98CH10886.

I. INTRODUCTION

The theory of high-gain single-pass free-electron lasers has been developing since the late 1970's [1-5]. In the absence of an external seed laser, the SASE FEL starts up from the shot noise in the electron beam. Because SASE starts from the shot noise, a proper theory requires a statistical treatment of the output radiation [6-17]. Average properties of the output were studied in [6-12] and fluctuations were considered in [13-17]. To describe the shot noise, one considers the arrival time of the individual electrons at the undulator entrance to be independent random variables, and one determines the statistical properties of the output radiation by averaging over the stochastic ensemble of arrival times. In the linear regime before saturation, it follows from the Central Limit Theorem [18] that the probability distribution describing the spectral intensity $I(\omega)$, or the time-domain intensity $I(t)$, is the negative exponential distribution [14]

$$p_I(I) = \frac{1}{\langle I \rangle} e^{-I/\langle I \rangle}, \tag{1.1}$$

and the intensity fluctuation is 100%.

The output intensity as a function of time exhibits spiking [13] (see Fig. 1), and the width of the intensity peaks is characterized by the coherence time [14,15], $T_{coh} = \sqrt{\pi}/\sigma_\omega$, where σ_ω is the SASE gain bandwidth. The spectral intensity also exhibits spikes (Fig. 2), and the width of the spectral peaks is inversely proportional to the electron bunch duration T_b.

At a fixed position z along the undulator, consider the energy in a single SASE pulse,

$$W(z) \propto \int_0^{T_b} |E(t,z)|^2 \, dt \ , \tag{1.2}$$

where T_b is the duration of an electron bunch having uniform average density. For z fixed, one can think of dividing the pulse into M statistically independent time-intervals of width T_{coh}. The energy fluctuation within a single coherent region is 100%, but the fluctuation σ_W / W of the energy in the entire pulse is reduced and given by [14,15]

$$\frac{\sigma_W^2}{W^2} = \frac{\left(W - \langle W \rangle\right)^2}{\langle W \rangle^2} \equiv \frac{1}{M} \equiv \frac{T_{coh}}{T_b} \ . \tag{1.3}$$

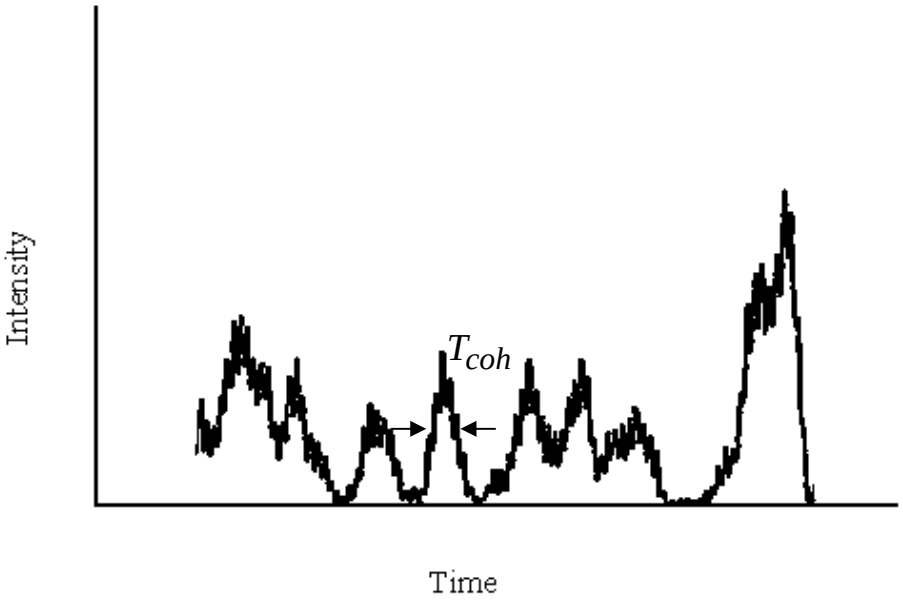

Figure 1. Intensity spiking in the time-domain (arbitrary units). The width of the peaks is characterized by the SASE coherence time $T_{coh} = \sqrt{\pi} / \sigma_{\omega}$.

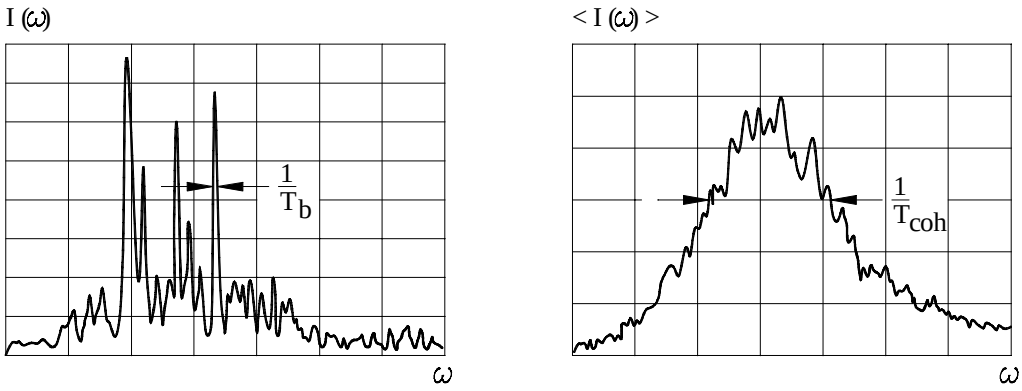

Figure. 2. Intensity spiking in the frequency-domain (arbitrary units). In the single-shot spectrum shown on the left, the width of the peaks is inversely proportional to the electron bunch duration T_b. The average of many SASE pulses is illustrated on the right, and in this case the width is proportional to the gain bandwidth $\sigma_{\omega} = \sqrt{\pi} / T_{coh}$.

Here, M is defined [14,19] to be the number of modes in the radiation pulse. The energy per pulse is described by the gamma distribution [14,18,19],

$$p_W(W) = \frac{M^M}{\Gamma(M)}\left(\frac{W}{\langle W\rangle}\right)^{M-1}\frac{1}{\langle W\rangle}\exp\left(-M\frac{W}{\langle W\rangle}\right). \tag{1.4}$$

Let $E(z,t) = A(z,t)\exp(ik_s z - i\omega_s t)$ be the radiated SASE electric field, where $\omega_s = k_s c$ is the undulator resonant frequency. In the description (at fixed z) of the statistical properties of the SASE output, two important quantities [14] are the field correlation function

$$g_1(t_1 - t_2) = \frac{\langle A(t_1)A^*(t_2)\rangle}{\sqrt{\langle |A(t_1)|^2\ |A(t_2)|^2\rangle}} \tag{1.5}$$

and the intensity correlation function

$$g_2(t_1 - t_2) = \frac{\langle |A(t_1)|^2 |A(t_2)|^2\rangle}{\langle |A(t_1)|^2\rangle\langle |A(t_2)|^2\rangle}. \tag{1.6}$$

In the linear region before saturation, they are related by

$$g_2(t) = 1 + |g_1(t)|^2\ . \tag{1.7}$$

The energy fluctuation σ_W in a pulse can be expressed in the form

$$\frac{\sigma_W^2}{W^2} = \frac{1}{T_b^2}\int_0^{T_b} dt_1 \int_0^{T_b} dt_2\,[g_2(t_1 - t_2) - 1] = \frac{1}{T_b}\int_{-T_b}^{T_b} dt\,|g_1(t)|^2\ . \tag{1.8}$$

Comparing Eqs. (1.3) and (1.8), we see that (when $T_{coh} << T_b$) the coherence time can be expressed in terms of the field correlation function according to [14,19]

$$T_{coh} = \int dt\,|g_1(t)|^2\ . \tag{1.9}$$

In this paper, we advance the statistical description of SASE by applying the mathematical analysis of random noise developed by Rice [18]. Some of the results of our analysis were presented in ref. [17]. In the earlier work [14] reviewed above, two important distributions of a "global" nature were derived: the exponential distribution [Eq. 1.1)] applies to an arbitrary time or frequency, and the gamma distribution applies to

the total radiated energy. In this paper, we study what might be termed "local" statistical properties. In the time-domain, we determine the joint probability [Eq.(3.14)] that at a fixed position z along the undulator axis, the normalized intensity $Q \equiv I / \langle I \rangle$ in the radiation pulse has the values Q_1 and Q_2 at times t_1 and t_2. We also find the probability per unit time [Eq. (4.10)] of observing a spike with maximum normalized intensity Q. In the frequency domain, we derive the joint probability [Eq. (3.21)] that the normalized spectral intensity has the values $\tilde{Q}_1$ and $\tilde{Q}_2$ at frequencies ω_1 and ω_2. We also find the probability per unit frequency interval [Eq. (4.18)] of observing a peak in the frequency spectrum with maximum normalized intensity $\tilde{Q}$.

In Eq. (1.3), the number of modes M in the output pulse was defined in terms of the pulse energy fluctuation. Another quantity of interest is the number of intensity spikes N_S (Fig. 1). Following Rice [18], we characterize the temporal spikes by the existence of local maxima of the intensity. From Eq. (4.14), we find that

$$N_S = 0.711M = 0.711T_b / T_{coh.} \ . \tag{1.10}$$

It is interesting to note that all known statistical properties of SASE derived in previous work [14] and in this paper can be derived from Rice's study [18] of shot noise in telephone systems, see also ref. [19].

Our paper is organized as follows: In Section II, we review the calculations of field and intensity correlations for the SASE radiation. In Section III, we use the Central limit theorem to determine the joint probability distributions mentioned above. In Section IV, we find the probability per unit time of observing a spike with maximum normalized intensity Q. From this result, we determine the average number of temporal spikes per unit time. We also find the probability per unit frequency interval of observing a peak in the frequency spectrum with maximum normalized intensity $\tilde{Q}$. From this result, we determine the average number of spectral spikes per unit frequency. In Section V, we present an approximate calculation of the probability per unit time of observing a spike with maximum normalized intensity Q>>1. This gives one an intuitive (albeit mathematical) picture of the spikes making up the SASE output. A summary of our results is given in Section VI.

II. CORRELATIONS

We work within the classical, one-dimensional approximation, in the linear regime before saturation. The uniform density electron bunch contains N_e electrons and has length, $L_b = cT_b$, long compared to the coherence length of the output radiation. We restrict our attention to the radiated field inside the electron bunch sufficiently far from the back end so that coherent effects [12,20,21] can be neglected. The radiation field has the form,

$$E(z,t) = A(z,t)\, e^{ik_s z - i\omega_s t} \quad , \tag{2.1}$$

with amplitude A given by

$$A(z,t) = \sum_{j=1}^{N_e} e^{i\omega_s \tau_j}\ h(z, t-\tau_j). \tag{2.2}$$

The resonant wavenumber $k_s = 2\gamma_0^2 k_w /(1+a_w^2),$ where k_w is the undulator wavenumber, $mc^2\gamma_0$ is the initial electron energy and a_w is the undulator strength parameter. The SASE green's function is denoted by $h(z,t)$ and the arrival time of the j^{th} electron at the undulator entrance (z=0) by τ_j. The independent random variables τ_j (j=1,…,N_e) are considered to be uniformly distributed over the interval $0 \le \tau_j \le T_b$.

We use brackets $\langle\ \rangle$ to represent an average over the arrival times. For the uniform distribution, $\left\langle f(\tau_j)\right\rangle = (N_e / T_b)\int_0^{T_b} d\tau\ f(\tau)$. We also introduce the shorthand notation: $A_1 = A(z,t_1)$ and $A_2 = A(z,t_2)$. The correlation of the amplitudes at a given position z along the undulator, at two different times is given by:

$$\begin{aligned}
\left\langle A_1 A_2^* \right\rangle &= \left\langle \sum_{j=1}^{N_e}\sum_{k=1}^{N_e} e^{-i\omega_s\tau_j} e^{i\omega_s\tau_k}\, h(t_1-\tau_j) h^*(t_2-\tau_k) \right\rangle \\
&\cong \sum_{j=1}^{N_e} h(t_1-\tau_j) h^*(t_2-\tau_j) \\
&\cong \frac{N_e}{T_b}\int_{-\infty}^{\infty} d\tau\ h(t_1-\tau) h^*(t_2-\tau)
\end{aligned} \tag{2.3}$$

In Eq. (2.3) and in the following, we do not explicitly show the z-dependence of the functions, since we are working at fixed z. While deriving Eq. (2.3), we retain only the dominant contributions characterized by the absence of rapid phase variation. These correspond to keeping pair-wise equal summation indices from the A and A^* terms.

It is often useful to introduce the Fourier transform $H(\Delta\omega)$, $\Delta\omega = \omega - \omega_s$, via

$$h(t) = \int \frac{d(\Delta\omega)}{2\pi} e^{i\Delta\omega t} H(\Delta\omega) . \tag{2.4}$$

The correlation of Eq. (2.3) can now be expressed as

$$\left\langle A_1 A_2^* \right\rangle \cong \frac{N_e}{T_b} \int \frac{d(\Delta\omega)}{2\pi} \left|H(\Delta\omega)\right|^2 e^{i\Delta\omega(t_1 - t_2)} \tag{2.5}$$

The correlation of the intensities at two different times can be calculated as follows:

$$\left\langle |A_1|^2 |A_2|^2 \right\rangle = \left\langle \sum_{jklm} e^{i\omega_s(-\tau_j + \tau_k - \tau_l + \tau_m)} h(t_1 - \tau_j) h^*(t_1 - \tau_k) h(t_2 - \tau_l) h^*(t_2 - \tau_m) \right\rangle$$

$$\cong \sum_{jl} \left|h(t_1 - \tau_j)\right|^2 \left|h(t_2 - \tau_l)\right|^2 + \sum_{jl} h(t_1 - \tau_j) h^*(t_2 - \tau_j) h^*(t_1 - \tau_l) h(t_2 - \tau_l)$$

$$= \left(\sum_j \left|h(t_1 - \tau_j)\right|^2 \right)^2 + \left| \sum_j h(t_1 - \tau_j) h*(t_2 - \tau_j) \right|^2$$

$$= \left\langle |A_1|^2 \right\rangle^2 + \left| \left\langle A_1 A_2^* \right\rangle \right|^2 . \tag{2.6}$$

This is the result of Eq. (1.7). Again we have kept only those terms without rapid phase variation.

Deep into the exponential gain regime, a saddle point analysis yields the Gaussian approximation to the green's function

$$h(k_w z, \theta) \cong e^{-i\pi/12} \frac{e^{(\sqrt{3}+i)\rho k_w z}}{\sqrt{8\pi\rho k_w z}} e^{-\frac{9\rho(\sqrt{3}+i)(\theta - \frac{k_w z}{3})^2}{4k_w z}}, \tag{2.7}$$

where $\theta = (k_s + k_w)z - \omega_s t$ and ρ is the Pierce parameter [3]. We can write this asymptotic approximation in the form

$$h(t) \cong \chi\, e^{-\alpha (t-\bar{t})^2} \quad , \tag{2.8}$$

where α and χ (complex) and $\bar{t}$ (real) are functions of z. From Eqs. (2.7) and (2.8), we see that

$$\alpha = \frac{9(\sqrt{3}+i)\omega_s^2 \rho}{4k_w z} \quad . \tag{2.9}$$

Taking the Fourier transform of (2.8), we find

$$\left|H(\Delta\omega)\right|^2 = \left|\chi\right|^2 \frac{\pi}{\sqrt{\alpha\alpha^*}} \quad e^{-(\Delta\omega)^2/2\sigma_\omega^2} , \tag{2.10}$$

$$\sigma_\omega^2 = \frac{2\alpha\alpha^*}{\alpha+\alpha^*} = \frac{3\sqrt{3}\rho\,\omega_s^2}{k_w z} \quad . \tag{2.11}$$

Here, σ_ω is the SASE gain bandwidth (see Fig. 2). Note that $H(\Delta\omega)$ has a dependence on ω_s that is not explicitly shown. Using the Gaussian approximation of Eq. (2.8) in Eq. (2.3) we derive

$$\left\langle A_1 A_2^* \right\rangle = \frac{N_e \left|\chi\right|^2}{T_b} \sqrt{\frac{\pi}{\alpha+\alpha^*}}\, e^{-\frac{\sigma_\omega^2}{2}(t_1-t_2)^2} . \tag{2.12}$$

We define the normalized amplitude,

$$a(z,t) = A(z,t) / \sqrt{\left\langle \left|A(z,t)\right|^2 \right\rangle} \quad , \tag{2.13}$$

and use the notation $a_1=a(z,t_1)$ and $a_2=a(z,t_2)$. Under the approximations we are employing,

$$\left\langle a_1 \right\rangle = \left\langle a_2 \right\rangle = \left\langle a_1 a_2 \right\rangle = 0 , \tag{2.14a}$$

$$\left\langle a_1 a_1^* \right\rangle = \left\langle a_2 a_2^* \right\rangle = 1, \quad \left\langle a_1 a_2^* \right\rangle \equiv u_{12} + i v_{12} , \tag{2.14b}$$

$$\left\langle \left|a_1\right|^2 \left|a_2\right|^2 \right\rangle \equiv 1 + \beta_{12} , \tag{2.14c}$$

$$\beta_{12} = \left|\left\langle a_1 a_2^* \right\rangle\right|^2 = u_{12}^2 + v_{12}^2 . \tag{2.14d}$$

Eqs. (2.14b) and (2.14c) provide the definitions of the quantities u_{12}, v_{12}, and β_{12}. We note that in terms of this notation, the field correlation introduced in Eq. (1.5) is given by

$g_1(t_1 - t_2) = \langle a_1 a_2^* \rangle$ and the intensity correlation introduced in Eq. (1.6) is $g_2(t_1 - t_2) = 1 + \beta_{12}$. In the high-gain regime before saturation, it follows from Eqs. (2.12), (2.13) and (2.14d) that

$$\beta_{12} = e^{-\pi (t_1 - t_2)^2 / T_{coh}^2}, \tag{2.15}$$

where T_{coh} [14,15] is the coherence time, which is related to the rms bandwidth σ_ω of the output SASE radiation by

$$T_{coh} = \frac{\sqrt{\pi}}{\sigma_\omega}. \tag{2.16}$$

III. JOINT PROBABILITY DISTRIBUTIONS

In Eq. (2.2), the amplitude A is represented as a sum of independent random terms; it follows that probability distributions describing the output radiation are determined from the Central Limit Theorem [18]. The central limit theorem (see Appendix A) states that the distribution P(V) of the normalized sum $V = (r_1 + r_2 + \cdots + r_N)/\sqrt{N}$ of N independent random vectors approaches the normal law as $N \to \infty$. For simplicity consider $\langle r_j \rangle = 0$; then as $N \to \infty$,

$$P(V) \to (2\pi)^{-K/2} (\det M)^{-1/2} \exp\left(-\frac{1}{2} V^T M^{-1} V \right), \tag{3.1}$$

where $V^T = (V_1, ..., V_K)$ is a K-dimensional row-vector (the superscript T indicates transpose) and V the corresponding column vector. The symmetric matrix M is comprised of the second moments:

$$M = \begin{bmatrix} \mu_{11} & \mu_{12} \cdots \mu_{1K} \\ \vdots & \\ \mu_{K1} & \mu_{K2} \cdots \mu_{KK} \end{bmatrix} \tag{3.2}$$

where

$$\mu_{jk} = \langle V_j V_k \rangle = \int d^K V \; (V_j V_k) \; P(V). \tag{3.3}$$

M^{-1} is the inverse of the matrix M. Note that when the central limit theorem applies, the distribution is Gaussian and hence is determined by the second moments. Under these

conditions, one need not compute all the higher moments to determine the distribution—a great simplification.

As an illustration, consider the special case when $r_1, r_2, ..., r_N$ are two-dimensional vectors with components, $r_j = (x_j, y_j)$. Again, we take $\langle x_j \rangle = \langle y_j \rangle = 0$ so independence implies $\langle x_j x_k \rangle = \langle y_j y_k \rangle = \langle x_j y_k \rangle = 0 \quad (j \neq k)$. The second moments of the resultant V=(X,Y) are:

$$\mu_{11} = \langle X^2 \rangle = \left\langle \frac{x_1^2 + \cdots + x_N^2}{N} \right\rangle , \tag{3.4}$$

$$\mu_{22} = \langle Y^2 \rangle = \left\langle \frac{y_1^2 + \cdots + y_N^2}{N} \right\rangle , \tag{3.5}$$

$$\mu_{12} = \mu_{21} = \langle XY \rangle = \left\langle \frac{x_1 y_1 + \cdots + x_N y_N}{N} \right\rangle . \tag{3.6}$$

In this case, the central limit theorem implies that the probability distribution P(X,Y) for $N \to \infty$ approaches the normal distribution

$$P(X,Y) = \frac{(\mu_{11}\mu_{22} - \mu_{12}^2)^{-1/2}}{2\pi} \exp\left[\frac{-\mu_{22} X^2 - \mu_{11} Y^2 + 2\mu_{12} XY}{2(\mu_{11}\mu_{22} - \mu_{12}^2)} \right]. \tag{3.7}$$

Returning to the FEL problem, let us express the normalized field amplitude defined in Eq. (2.13) as

$$a = x + iy = \sqrt{Q} e^{i\phi}. \tag{3.8}$$

Correlations of x and y are determined from Eqs. (2.14) and one finds: $\langle x^2 \rangle = \langle y^2 \rangle = 1/2$ and $\langle xy \rangle = 0$. From the Central Limit Theorem, it is seen that the probability P(x,y)dxdy for finding x between x and x+dx, and y between y and y+dy, is given by

$$P(x, y) = \frac{1}{\pi} e^{-x^2 - y^2} . \tag{3.9}$$

The probability $P(Q, \phi)dQd\phi$ for finding Q between Q and Q+dQ, and ϕ between ϕ and $\phi + d\phi$, is given by

$$P(Q,\phi) = \frac{1}{2\pi} e^{-Q}. \tag{3.10}$$

As shown by Rice [18], the Central Limit Theorem also enables us to determine the joint probability distribution describing the field amplitudes at two different times. The required correlations are determined from Eqs. (2.14), and we find: $\langle x_1^2 \rangle = \langle x_2^2 \rangle = \langle y_1^2 \rangle = \langle y_2^2 \rangle = 1/2$, $\langle x_1 y_1 \rangle = \langle x_2 y_2 \rangle = 0$, $\langle x_1 x_2 \rangle = \langle y_1 y_2 \rangle = u_{12}/2$, and $\langle x_1 y_2 \rangle = -\langle y_1 x_2 \rangle = v_{12}/2$. Taking the vector $V^T = (x_1, y_1, x_2, y_2)$, the moment matrix M introduced in Eq. (3.2) and its inverse are given by

$$M = \frac{1}{2}\begin{bmatrix} 1 & 0 & u_{12} & v_{12} \\ 0 & 1 & -v_{12} & u_{12} \\ u_{12} & -v_{12} & 1 & 0 \\ v_{12} & u_{12} & 0 & 1 \end{bmatrix}, \tag{3.11}$$

$$M^{-1} = \frac{2}{1-u_{12}^2-v_{12}^2}\begin{bmatrix} 1 & 0 & -u_{12} & -v_{12} \\ 0 & 1 & v_{12} & -u_{12} \\ -u_{12} & v_{12} & 1 & 0 \\ -v_{12} & -u_{12} & 0 & 1 \end{bmatrix}. \tag{3.12}$$

Also, one finds $\det M = (1-u_{12}^2-v_{12}^2)^2$. It then follows from Eqs. (3.1) and (3.12) that

$$P(x_1, y_1, x_2, y_2) = \frac{1}{\pi^2(1-\beta_{12})} \exp\left(\frac{-x_1^2 - y_1^2 - x_2^2 - y_2^2 - 2u_{12}(x_1x_2 + y_1y_2) - 2v_{12}(x_1y_2 - y_1x_2)}{(1-\beta_{12})} \right). \tag{3.13}$$

Expressing x and y in terms of Q and ϕ via Eq. (3.8), and integrating over ϕ_1 and ϕ_2, we obtain the probability $P(Q_1,Q_2)dQ_1dQ_2$ for finding normalized intensity between Q_1 and Q_1+dQ_1 at time t_1, and Q_2 and Q_2+dQ_2 at time t_2 [18]:

$$P(Q_1, Q_2) = \frac{e^{\frac{-Q_1}{1-\beta_{12}}} e^{\frac{-Q_2}{1-\beta_{12}}}}{1-\beta_{12}} I_0\left(\frac{2\sqrt{\beta_{12} Q_1 Q_2}}{1-\beta_{12}} \right). \tag{3.14}$$

I_0 is the Bessel function of imaginary argument of order zero. Note that when $t_1 \to t_2$, then $\beta_{12} \to 1$ and $P(Q_1, Q_2) \to e^{-Q_1}\delta(Q_1 - Q_2)$. Also, when $|t_1 - t_2| \to \infty$, then $\beta_{12} \to 0$

and $P(Q_1, Q_2) \to e^{-Q_1 - Q_2}$. The distribution of Eq. (3.14) has been used to describe narrow band chaotic light [22]. Some mathematical properties of the distribution have been studied in [23], where the following expansion in terms of Laguerre polynomials was derived

$$P(Q_1, Q_2) = e^{-Q_1} e^{-Q_2} \sum_{n=0}^{\infty} \beta_{12}^{\,n} L_n(Q_1) L_n(Q_2) . \tag{3.15}$$

From Eq. (3.15), one can calculate the moments

$$\begin{aligned} \left\langle Q_1^M Q_2^N \right\rangle &= \int_0^{\infty} dQ_1 \int_0^{\infty} dQ_2 \; Q_1^M Q_2^N \; P(Q_1, Q_2) \\ &= M! N! \sum_{k=0}^{\min(M,N)} \frac{M!}{k!(M-k)!} \frac{N!}{k!(N-k)!} \beta_{12}^{\,k} . \end{aligned} \tag{3.16}$$

It is now of interest to determine the conditional average $\left\langle Q_2 \right\rangle_{Q_1}$ of the intensity at t_2, given the intensity at t_1 is Q_1.

$$\left\langle Q_2 \right\rangle_{Q_1} = \frac{\int_0^{\infty} dQ_2 \; Q_2 \; P(Q_1, Q_2)}{\int_0^{\infty} dQ_2 \; P(Q_1, Q_2)} = Q_1 + (1 - \beta_{12})(1 - Q_1) . \tag{3.17}$$

The corresponding fluctuation is

$$\left\langle Q_2^2 \right\rangle_{Q_1} - \left\langle Q_2 \right\rangle_{Q_1}^2 = 2 Q_1 \beta_{12} (1 - \beta_{12}) + (1 - \beta_{12})^2 . \tag{3.18}$$

We note from Eq. (3.17) that $\left\langle Q_2 \right\rangle_{Q_1}$ is less than Q_1 when $Q_1 > 1$, and is greater than Q_1 when $Q_1 < 1$. This is the statistical basis for the appearance of spikes in the radiation output.

The analysis just presented in the time-domain can be extended into the frequency-domain. Let $\tilde{A}(z, \Delta\omega)$ be the Fourier transform of A(z,t), where $\Delta\omega = \omega - \omega_s$. Then

$$\tilde{A}(z, \Delta\omega) = H(z, \Delta\omega) \sum_{j=1}^{N_e} e^{-i(\omega_s + \Delta\omega)\tau_j} , \tag{3.19}$$

where H is the Fourier transform of h, $|H(z,\Delta\omega)|^2 = |H_0(z)|^2 \exp[-(\Delta\omega)^2/2\sigma_\omega^2]$. From Eq. (3.19), we find

$$\left\langle \tilde{A}(\Delta\omega_1)\tilde{A}^*(\Delta\omega_2)\right\rangle = H(\Delta\omega_1)H^*(\Delta\omega_2)\sum_{jk}\left\langle e^{-i(\omega_s+\Delta\omega_1)\tau_j} e^{i(\omega_s+\Delta\omega_2)\tau_k}\right\rangle$$

$$\cong H(\Delta\omega_1)H^*(\Delta\omega_2)\sum_j e^{i(\Delta\omega_2-\Delta\omega_1)\tau_j}$$

$$\cong H(\Delta\omega_1)H^*(\Delta\omega_2)\frac{N_e}{T_b}\int_{-T_b/2}^{T_b/2} d\tau\, e^{i(\Delta\omega_2-\Delta\omega_1)\tau}$$

$$= H(\Delta\omega_1)H^*(\Delta\omega_2)N_e \operatorname{sinc}\left(\frac{T_b}{2}(\Delta\omega_2-\Delta\omega_1)\right). \qquad (3.20)$$

We define, $\tilde{a}(\Delta\omega) = \tilde{A}(z,\Delta\omega)/\sqrt{\left\langle\left|\tilde{A}(z,\Delta\omega)\right|^2\right\rangle}$, $\tilde{Q}(\Delta\omega) = \left|\tilde{a}(\Delta\omega)\right|^2$, and $\tilde{Q}_1 = \tilde{Q}(\Delta\omega_1)$, $\tilde{Q}_2 = \tilde{Q}(\Delta\omega_2)$. The joint probability $P(\tilde{Q}_1,\tilde{Q}_2)d\tilde{Q}_1\, d\tilde{Q}_2$ that the normalized spectral intensities at frequencies ω_1 and ω_2 have values between $\tilde{Q}_1$ and $\tilde{Q}_1 + d\tilde{Q}_1$, and $\tilde{Q}_2$ and $\tilde{Q}_2 + d\tilde{Q}_2$, respectively, is determined in a manner similar to the derivation in the time-domain leading to Eq. (3.14). We find,

$$P(\tilde{Q}_1,\tilde{Q}_2) = \frac{e^{\frac{-\tilde{Q}_1}{1-\gamma_{12}}} e^{\frac{-\tilde{Q}_2}{1-\gamma_{12}}}}{1-\gamma_{12}} I_0\left(\frac{2\sqrt{\gamma_{12}\tilde{Q}_1\tilde{Q}_2}}{1-\gamma_{12}}\right), \qquad (3.21)$$

where

$$\gamma_{12} = \left\langle \tilde{Q}_1\tilde{Q}_2\right\rangle - 1 = \left|\left\langle \tilde{a}_1\tilde{a}_2^*\right\rangle\right|^2 = \operatorname{sinc}^2\left(\frac{(\omega_1-\omega_2)T_b}{2}\right), \qquad (3.22)$$

and sinc(x)=(sin x)/x. As in the time-domain, it is possible to write Eq. (3.21) in terms of Laguerre polynomials.

IV. INTENSITY PEAKS

We can provide a statistical description of the spikes in the output, first in the time-domain and then in the frequency-domain. To prepare for the discussion of the intensity peaks, we first review the required mathematics developed by Rice [18]. Consider the stochastic function

$$y = F(\tau_1, \tau_2, ..., \tau_N; t) \tag{4.1}$$

and its derivative

$$y' = \frac{\partial F}{\partial t}, \tag{4.2}$$

where $\tau_1, ..., \tau_N$ are random variables. Let $P(\xi, \eta; t) d\xi\, d\eta$ be the probability of finding y between ξ and $\xi + d\xi$, and y' between η and $\eta + d\eta$ at time t. We first wish to determine the probability that there is a zero of the function F having positive slope somewhere in the interval $t_1 < t < t_1 + dt$. Suppose $y = \xi < 0$ at t_1 and y=0 somewhere in $t_1 < t < t_1 + dt$. If the slope at t_1 is $\eta > 0$, then F passes through zero at $t = t_1 - \frac{\xi}{\eta}$. Hence, we require $t_1 < t_1 - \frac{\xi}{\eta} < t_1 + dt$, i.e. $-\eta dt < \xi < 0$. Therefore, the probability that there is a zero of F with positive slope in $t_1 < t < t_1 + dt$ is given by

$$\int_0^\infty d\eta \int_{-\eta dt}^0 d\xi P(\xi, \eta; t_1) = dt \int_0^\infty \eta d\eta P(0, \eta; t_1). \tag{4.3}$$

We can now determine the probability $p(y_1)dtdy$ that F has a maximum with value between y_1 and y_1+dy in the time interval $t_1<t<t_1+dt$. At a maximum, the derivative of F is zero and its second derivative is negative. From the result of Eq.(4.3), we see that

$$p(y_1; t_1) dt dy = -dt dy \int_{-\infty}^0 \varsigma d\varsigma P(y_1, 0, \varsigma; t_1), \tag{4.4}$$

where $P(\xi, \eta, \varsigma; t_1)$ is the probability density function for the variables $\xi = F(\tau_1, ..., \tau_N; t_1)$, $\eta = \left(\partial F / \partial t\right)_{t=t_1}$, and $\varsigma = \left(\partial^2 F / \partial t^2\right)_{t=t_1}$.

Let $a^{(m)} = \partial^m a / \partial t^m$ and note that

$$\left\langle a^{(m)} a^{(n)*} \right\rangle = 2 i^{m-n} b_{m+n}, \tag{4.5}$$

$$b_m = K(z) \int_{-\infty}^{\infty} \frac{d(\Delta\omega)}{2\pi} \left| H(z, \Delta\omega) \right|^2 (\Delta\omega)^m. \tag{4.6}$$

The normalization K(z) is chosen so that b_0=1/2. We write $a = x + iy$, $a' = x' + i\,y'$, $a'' = x'' + i\,y''$, where the prime denotes differentiation with respect to time t. Using the Central Limit Theorem, Rice [18] determines $P(x, y, x', y', x'', y'')$. Taking $V^T = (x, y', x'', y, x', y'')$, the matrix M of second moments, Eq. (3.2), is

$$M = \begin{bmatrix} b_0 & b_1 & -b_2 & 0 & 0 & 0 \\ b_1 & b_2 & -b_3 & 0 & 0 & 0 \\ -b_2 & -b_3 & b_4 & 0 & 0 & 0 \\ 0 & 0 & 0 & b_0 & -b_1 & -b_2 \\ 0 & 0 & 0 & -b_1 & b_2 & b_3 \\ 0 & 0 & 0 & -b_2 & b_3 & b_4 \end{bmatrix} \tag{4.7}$$

After computing the inverse of M, $P(x, y, x', y', x'', y'')$ is determined from Eq. (3.1). Rice then introduces $x = R\cos\phi, y = R\sin\phi$, and takes the first and second time derivatives. By integrating over $\phi, \phi', and\ \phi''$, Rice determines $P(R, R', R'')$. He then notes that the probability p_t(R) dtdR that a maximum of the envelope R falls within the elementary rectangle dtdR is given by [see Eq. (4.4)]

$$p_t(R) = -\int_{-\infty}^{0} P(R, 0, R'')\, R''\, d\, R''. \tag{4.8}$$

independent of t. We use the variable $Q=R^2$, and we choose the normalization K(z) such that

$$K(z)\left|G(z, \Delta\omega)\right|^2 = \frac{1}{2\sqrt{2\pi}\sigma_\omega} e^{-(\Delta\omega)^2/2\sigma_\omega^2}\ . \tag{4.9}$$

The probability $p_t(Q)dtdQ$ that a maximum of Q with value between Q and Q+dQ is found in time interval dt is determined by [18],

$$p_t(Q) = \frac{1}{4T_{coh}} (2Q)^{1/4} e^{-3Q/2} \sum_{n=0}^{\infty} \frac{(n+1)(Q/2)^{n/2}}{\Gamma(\frac{n}{2} + \frac{7}{4})}. \tag{4.10}$$

For Q>>1, the sum over n in (4.10) clearly peaks near n=Q. One can treat n as a continuous variable, convert the sum over n to an integral and use the method of steepest descent to obtain

$$p_t(Q) \approx \frac{1}{T_{coh}} e^{-Q} \sqrt{Q} \left(1 - \frac{1}{2Q}\right). \tag{4.11}$$

Another method for evaluating the sum over n in (4.10) for large Q is to separate it into two pieces

$$\sum_{n=0}^{\infty} \frac{(n+1)(Q/2)^{n/2}}{\Gamma(\frac{n}{2}+\frac{7}{4})} = 2\sum_{n=0}^{\infty} \frac{(Q/2)^{n/2}}{\Gamma(\frac{n}{2}+\frac{3}{4})} - \frac{1}{2}\sum_{n=0}^{\infty} \frac{(Q/2)^{n/2}}{\Gamma(\frac{n}{2}+\frac{7}{4})} \quad . \tag{4.12}$$

Summing over alternate values of n and recognizing that the lower limit n=0 in the sums can be modified slightly without affecting the overall limit as $Q \to \infty$, one obtains the asymptotic approximation of Eq. (4.11) by noting that

$$\sum_{m=0}^{\infty} \frac{(Q/2)^m}{\Gamma(m+1)} = e^{Q/2} \quad . \tag{4.13}$$

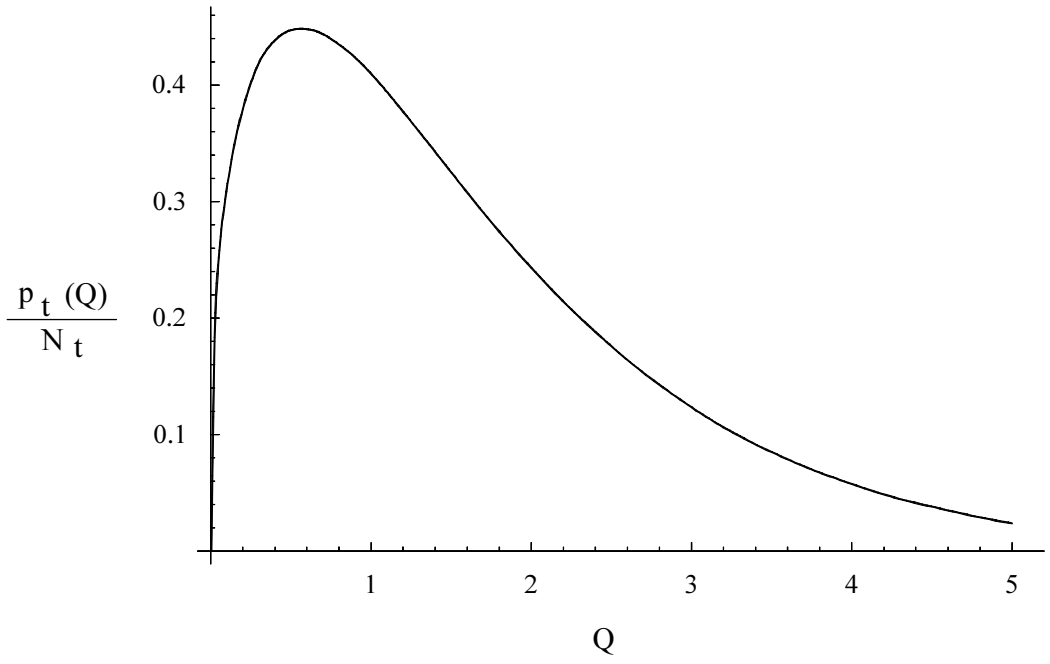

Figure. 3. $p_t(Q)/N_t$ dQ is the probability of a peak in the time-domain having normalized intensity between Q and Q+dQ (dimensionless variables).

The number of peaks per unit time is

$$N_t = \int_0^{\infty} dQ\, p_t(Q) = \frac{0.711}{T_{coh}}. \tag{4.14}$$

The probability of finding a maximum with normalized intensity between Q and Q+dQ is $p_t(Q)/N_t\ dQ$, which is plotted in Fig. 3. The average peak height is $\langle Q \rangle = 1.56$ and the rms peak height fluctuation is 1.27. In Eq. (4.14) and Fig. 3, $p_t(Q)$ is determined from Eq. (4.10).

In the frequency domain,

$$\tilde{a}(\Delta\omega) = \frac{1}{\sqrt{N_e}} \sum_{j=1}^{N_e} e^{-i(\omega_s + \Delta\omega)\tau_j} \ . \tag{4.15}$$

Defining $\tilde{a}^{(m)} = \partial^m \tilde{a} / \partial\omega^m$, we find

$$\left\langle \tilde{a}^{(m)} \ \tilde{a}^{(n)*} \right\rangle = 2i^{n-m} b_{m+n} , \tag{4.16}$$

$$b_m = \frac{1}{2T_b} \int_{-T_b/2}^{T_b/2} dt\, t^m \ . \tag{4.17}$$

Following Rice's analysis [18], we find that the probability $p_\omega(\tilde{Q}) d\omega d\tilde{Q}$ that a maximum of $\tilde{Q} = \left|\tilde{a}\right|^2$ with value between $\tilde{Q}$ and $\tilde{Q} + d\tilde{Q}$ is observed in frequency interval dω is determined by

$$p_\omega(\tilde{Q}) = \frac{T_b/2\pi}{4} \sqrt{\frac{\pi}{6}}\ \tilde{Q}^{1/4}\ e^{-9\tilde{Q}/4} \sum_{n=0}^{\infty} \frac{(5/4)^{n/2-3/4} \tilde{Q}^{n/2} A_n}{\Gamma(\frac{n}{2} + \frac{7}{4})} , \tag{4.18}$$

independent of ω, with

$$A_0 = 1, \tag{4.19a}$$

$$A_n = \sum_{m=0}^{n} \frac{(1/2)(3/2)\cdots(m-1/2)}{m!} (n-m+1)(3/5)^m , \quad (n \geq 1) \ . \tag{4.19b}$$

For $\tilde{Q} >> 1$,

$$p_\omega(\tilde{Q}) \approx \frac{T_b}{2\pi} \sqrt{\frac{\pi}{3}}\ e^{-\tilde{Q}} \sqrt{\tilde{Q}} \left(1 - \frac{1}{2\tilde{Q}} \right). \tag{4.20}$$

The number of peaks per unit frequency is

$$N_\omega = \int_0^\infty d\tilde{Q}\ p_\omega(\tilde{Q}) = 0.641 (T_b / 2\pi) . \tag{4.21}$$

The probability of finding a maximum with normalized spectral intensity between $\tilde{Q}$ and $\tilde{Q}+d\tilde{Q}$ is $p_\omega(\tilde{Q})/N_\omega\, d\tilde{Q}$, which is plotted in Fig. 4. The average spectral peak height is $\left\langle \tilde{Q} \right\rangle = 1.66$ and the rms spectral peak height fluctuation is 1.29. In Eq. (4.21) and Fig. 4, $p_\omega\left(\tilde{Q}\right)$ is determined from Eq. (4.18).

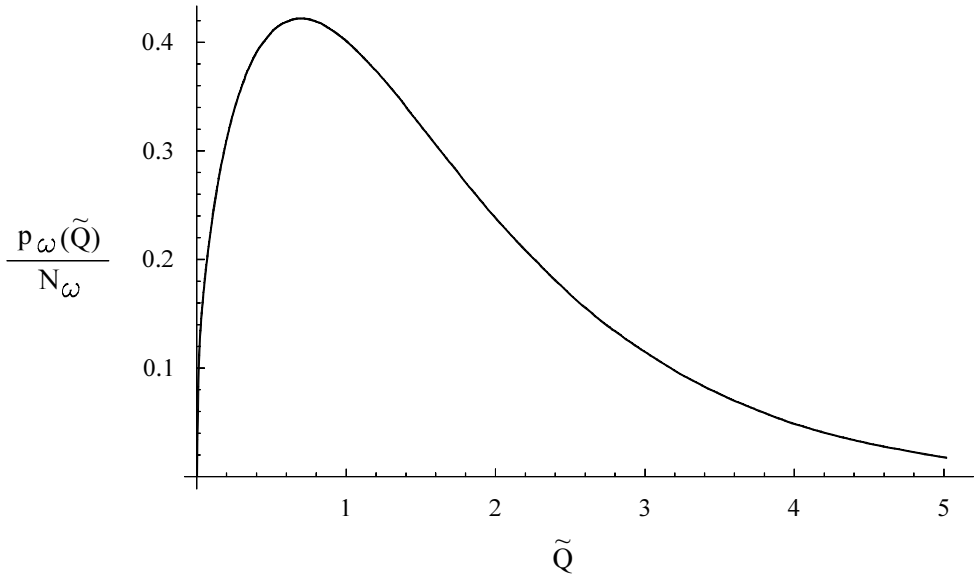

Figure. 4. $p_\omega(\tilde{Q})/N_\omega\, d\tilde{Q}$ is the probability of a peak in the frequency-domain having normalized intensity between $\tilde{Q}$ and $\tilde{Q}+d\tilde{Q}$ (dimensionless variables).

V. APPROXIMATE DESCRIPTION OF INTENSITY SPIKES

Motivated by the result for the conditional average, Eq. (3.17), it is reasonable to assume that the output is comprised of a series of peaks, and in the region near each maximum, the intensity profile can be approximated by

$$Q = Q_p e^{-\pi (t-t_p)^2 / T_{coh}^2}, \tag{5.1}$$

where Q_p is the maximum intensity of the peak centered about $t=t_p$.

Recall from Section IV that $p_t(Q)dQdt$ is the probability of finding in the radiation output an intensity peak of magnitude between Q and Q+dQ, in time interval dt. Let us

consider an intuitive argument for determining the large Q behavior of $p_t(Q)$. For large Q_1, the probability of the intensity Q being greater than Q_1 can be evaluated in two ways. First, it is equal to $\int_{Q_1}^{\infty} dQ\, e^{-Q} = e^{-Q_1}$. Alternatively, it can be written as $\int_{Q_1}^{\infty} dQ\; p_t(Q)\, \Delta t(Q, Q_1)$, where $\Delta t(Q, Q_1)$ represents the region in t, under a peak having maximum value Q, for which the intensity is greater than Q_1. From Eq. (5.1), we find $\Delta t(Q, Q_1) = 2T_{coh}\sqrt{\frac{\ell n(Q/Q_1)}{\pi}}$. Equating these two expressions for the probability that the intensity Q be greater than Q_1, we derive the following integral equation for $p_t(Q)$:

$$\int_{Q_1}^{\infty} dQ\; p_t(Q)\, 2T_{coh}\sqrt{\frac{\ell n(Q/Q_1)}{\pi}} \quad = \quad e^{-Q_1}. \tag{5.2}$$

For large Q_1, the exponential behavior on the right hand side of Eq. (5.2) requires that $p_t(Q) \to e^{-Q}F(Q)$. If one changes the variable of integration to $y=Q-Q_1$, then Eq. (5.2) becomes

$$\frac{2T_{coh}}{\sqrt{\pi}}\int_0^{\infty} dy\, e^{-y}\; F(Q_1+y)\sqrt{\ell n(1+\frac{y}{Q_1})} = 1 \tag{5.3}$$

Clearly, the important values of y are of the order of 1. Thus, for large Q_1, one has $y \ll Q_1$ and $\sqrt{\ell n(1+\frac{y}{Q_1})} \cong \sqrt{\frac{y}{Q_1}}(1-\frac{y}{4Q_1})$. Expanding $F(Q_1+y)$ for $y \ll Q_1$ leads to

$$\frac{2T_{coh}}{\sqrt{\pi}}\int_0^{\infty} dy\, e^{-y}\left[F(Q_1)+yF'(Q_1)\right]\left[\frac{y^{1/2}}{Q_1^{1/2}}-\frac{y^{3/2}}{4Q_1^{3/2}}\right] \cong 1 \quad . \tag{5.4}$$

The solution of (5.4) for large Q_1 is $F(Q_1) \cong \frac{1}{T_{coh}}\sqrt{Q_1}\,(1-\frac{3}{8Q_1})$. Thus the solution of Eq. (5.2) for large Q is

$$p_t(Q) \cong \frac{1}{T_{coh}}\, e^{-Q}\, \sqrt{Q}\,(1-\frac{3}{8Q}). \tag{5.5}$$

We see that the intuitive argument leads to a result differing from the precise asymptotic result of Eq. (4.11) only in that the factor 3/8 should be replaced by 1/2.

Let us extend the intuitive picture and suppose the output intensity is comprised of a sum of peaks,

$$Q(t) \cong \sum_p Q_p e^{-\pi (t-t_\ell)^2 / T_{coh}^2}\ , \tag{5.6}$$

where now we do not restrict Q_p to be large. Then we can approximate the average value of Q(t) by [see Eq. (4.14) and the discussion following it]

$$\langle Q(t) \rangle \cong \int_0^\infty dQ_p \int_{-\infty}^\infty dt_p\ p_t(Q_p) Q_p e^{-\pi (t-t_p)^2 / T_{coh}^2} \cong N_t \langle Q_p \rangle T_{coh} = \frac{0.711}{T_{coh}} (1.56) T_{coh} = 1.1, \tag{5.7}$$

in reasonable agreement with the exact value, 1, of this average. Similarly, let us consider the output intensity spectrum to be comprised of a sum of peaks

$$\tilde{Q}(\omega) \cong \sum_\ell \tilde{Q}_\ell\ \mathrm{sinc}^2\left(\frac{(\omega - \omega_\ell) T_b}{2} \right). \tag{5.8}$$

We can approximate the average of $\tilde{Q}(\omega)$ by [see Eq. (4.21) and the discussion following it]

$$\left\langle \tilde{Q}(\omega) \right\rangle \cong \int_0^\infty d\tilde{Q}_\ell \int_{-\infty}^\infty d\omega_\ell\ p_\omega(\tilde{Q}_\ell) \tilde{Q}_\ell\ \mathrm{sinc}^2\left(\frac{(\omega - \omega_\ell) T_b}{2} \right) \cong N_\omega \left\langle \tilde{Q}_\ell \right\rangle \frac{2\pi}{T_b}$$

$$= 0.641 \frac{T_b}{2\pi} (1.66) \frac{2\pi}{T_b} = 1.06\,, \tag{5.9}$$

also in reasonable agreement with the exact value, 1.

VI. SUMMARY OF RESULTS

In this paper, we have used the approach of Rice [18] to extend our knowledge of SASE statistics. In earlier work [14], it was shown that the probability distribution for the intensity at a given time or frequency is the exponential distribution [Eq. (1.1)]. The field correlation $g_1(t_1 - t_2)$ [Eq. (1.5)] and intensity correlation $g_2(t_1 - t_2)$ [Eq. (1.6)] were also determined [14], as well as the gamma distribution [Eq. (1.4)] for the energy per pulse. In this paper, we have derived the joint probability $P(Q_1,Q_2)dQ_1dQ_2$ for finding normalized intensity between Q_1 and Q_1+dQ_1 at time t_1, and Q_2 and Q_2+dQ_2 at time t_2 :

$$P(Q_1,Q_2) \;=\; \frac{e^{\frac{-Q_1}{1-\beta_{12}}}e^{\frac{-Q_2}{1-\beta_{12}}}}{1-\beta_{12}}\, I_0\left(\frac{2\sqrt{\beta_{12}Q_1Q_2}}{1-\beta_{12}}\right), \tag{6.1}$$

where $\beta_{12} = \langle Q_1 Q_2 \rangle - 1 \cong e^{-\pi(t_1-t_2)^2/T_{coh}^2}$. In addition, we have determined the joint probability $P(\tilde{Q}_1,\tilde{Q}_2)d\tilde{Q}_1\, d\tilde{Q}_2$ that the normalized spectral intensities at frequencies ω_1 and ω_2 have values between $\tilde{Q}_1$ and $\tilde{Q}_1 + d\tilde{Q}_1$, and $\tilde{Q}_2$ and $\tilde{Q}_2 + d\tilde{Q}_2$:

$$P(\tilde{Q}_1,\tilde{Q}_2) \;=\; \frac{e^{\frac{-\tilde{Q}_1}{1-\gamma_{12}}}e^{\frac{-\tilde{Q}_2}{1-\gamma_{12}}}}{1-\gamma_{12}}\, I_0\left(\frac{2\sqrt{\gamma_{12}\tilde{Q}_1\tilde{Q}_2}}{1-\gamma_{12}}\right), \tag{6.2}$$

where $\gamma_{12} = \left\langle \tilde{Q}_1 \tilde{Q}_2 \right\rangle - 1 = \mathrm{sinc}^2\left(\frac{(\omega_1-\omega_2)T_b}{2}\right)$.

In the time-domain (Fig. 1), we have derived the probability $p_t(Q)/N_t\, dQ$ [Eq. (4.10) and Fig. 3] of finding a maximum with normalized intensity between Q and Q+dQ. The number of peaks per unit time was found to be

$$N_t = 0.711/T_{coh}. \tag{6.3}$$

In frequency domain (Fig. 2), we have determined the probability $p_\omega(\tilde{Q})/N_\omega\, d\tilde{Q}$ [Eq. (4.18) and Fig. 4] of finding a maximum with normalized spectral intensity between $\tilde{Q}$ and $\tilde{Q} + d\tilde{Q}$. The number of peaks per unit frequency was found to be

$$N_\omega = 0.641(T_b/2\pi). \tag{6.4}$$

Many of the statistical properties of the radiation reviewed in the introduction to this paper have been verified experimentally [24]. In particular, it was observed that the fluctuations of the SASE radiation energy followed the gamma distribution [Eq. (1.4)], and the output of a narrow-band monochromator behaved as expected from theory. Spikes in the spectral distribution of intensity have been measured experimentally [25-27]. If experimental conditions are sufficiently controlled so that fluctuations are dominated by shot noise and not variations in experimental parameters such as charge, bunch length or emittance, then the distribution of peak heights can be measured and compared with the prediction of Eq. (4.18). Also, one can compare the number of peaks

per unit frequency with the prediction of Eq. (6.4). In the future, if one develops methods to directly measure spikes in the time domain, then the predictions of Eqs. (4.10) and (6.3) can be compared with experiment.

ACKNOWLEDGEMENTS

This work was supported by Department of Energy contracts DE–AC03–76SF00515 and DE-AC02-98CH10886.

REFERENCES

[1] N.M. Kroll and W.A. McMullin, Phys. Rev. **A17** (1978) 300.

[2] Y.S. Debenev, A.M. Kondratenko and E.L. Saldin, Nucl. Instrum Methods Phys. Res **A193** (1982) 415.

[3] R. Bonifacio, C. Pellegrini, and L.M. Narducci, Opt. Commun. **50** (1984) 373.

[4] L.H. Yu, S. Krinsky, R.L. Gluckstern, Phys. Rev Lett. **64** (1990) 3011.

[5] M. Xie, Nucl. Instrum. Meth. **A445**, 59 (2000).

[6] J.M. Wang and L.H. Yu, Nucl. Instrum. Meth. **A250** (1986) 484.

[7] K.J. Kim, Nucl. Instrum. Meth. **A250** (1986) 396.

[8] K.J. Kim, Phys. Rev. Lett. **57** (1986) 1871.

[9] S. Krinsky, AIP Conf. Proc. **153** (1987) 1015.

[10] S. Krinsky and L.H. Yu, Phys. Rev. **35** (1987) 3406.

[11] L.H. Yu and S. Krinsky, Nucl. Instrum. Meth. **A285** (1989) 119.

[12] S. Krinsky, Phys. Rev. **E59** (1999) 1171.

[13] R. Bonifacio, L. De Salvo, P Pierini, N. Piovella, and C. Pellegrini, Phys. Rev. Lett. **73** (1994) 70.

[14] E.L. Saldin, E.A. Schneidmiller, M.V. Yurkov, *The Physics of Free Electron Lasers*, Springer-Verlag, Berlin, 2000, Chapter 6.

[15] L. H. Yu and S. Krinsky, Nucl. Instrum. Meth. **A407** (1998) 261.

[16] P. Catravas et al., Phys. Rev. Lett. **82** (1999) 5261.

[17] S. Krinsky and R.L. Gluckstern, in Proc. 23rd International Free-Electron Laser Conference, Darmstadt, August 20-24, 2001; Nucl. Instrum. Meth. **A483**, 57 (2002).

[18] S.O Rice, Bell System Technical Journal **24** (1945) 46.

[19] J.W. Goodman, *Statistical Optics*, John Wiley & Sons, New York (1985).

[20] B.W.J. McNeil, G.R.M. Robb, D.A. Jaroszynski, Opt. Commun. **165** (1999) 65.

[21] Z Huang and K.J. Kim, Nucl. Instrum. Meth. **A445** (2000) 105.

[22] G. Vannucci and M.C. Teich, J. Opt. Soc. Am. **71** (1981) 164.

[23] J.F. Barrett and D.G. Lampard, IRE Trans.-Information Theory **IT-1** (1955) 10.

[24] M.V. Yurkov et al., Nucl. Instrum. Meth. **A483 (2002)** 51.

[25] Ayvazyan et al, Phys. Rev. Lett. **88**, 104802 (2002).

[26] S.V. Milton et al, Science **292**, 2037 (2001).

[27] A. Tremaine et al, Nucl. Instrum. Meth. **A483** (2002) 51.

APPENDIX A: CENTRAL LIMIT THEOREM

Since the central limit theorem plays a central role in our analysis, we shall provide a short heuristic derivation of this important result. Let us consider N independent random variables $x_1,\ldots,x_N$ satisfying $\left\langle x_j \right\rangle = 0$, $\left\langle x_j x_k \right\rangle = \sigma^2 \delta_{jk}$. Then in the limit $N \to \infty$, we wish to determine the distribution of the normalized sum

$$S = \frac{1}{\sqrt{N}} \sum_{j=1}^{N} x_j \tag{A1}$$

For $N \to \infty$,

$$\left\langle e^{i\omega S} \right\rangle = \left\langle \exp\left(i\omega \frac{1}{\sqrt{N}} \sum_{j=1}^{N} x_j \right) \right\rangle \cong \left(1 - \frac{\omega^2 \sigma^2}{2N} \right)^N \cong e^{-\omega^2 \sigma^2 / 2} \quad . \tag{A2}$$

By definition,

$$\left\langle e^{i\omega S} \right\rangle = \int dS \; p(S) e^{i\omega S} \quad . \tag{A3}$$

Taking the inverse Fourier transform, it follows from Eqs. (A2) and (A3) that

$$p(S) = \frac{1}{\sqrt{2\pi}\sigma} \quad e^{-S^2 / 2\sigma^2} , \tag{A4}$$

a special case of the central limit theorem.

APPENDIX B. THE SPECTRAL DENSITY

The real electric field ε is expressed in terms of the complex amplitude A by

$$\varepsilon(z,t) = \frac{1}{2} A(z,t) e^{ik_s z - i\omega_s t} + c.c\,, \tag{B1}$$

Since we consider z fixed and are only concerned with the time dependence, we shall write $\varepsilon(t)$ and $A(t)$, ignoring the functional dependence on z. It then follows that

$$\langle \varepsilon(t_1)\varepsilon(t_2)\rangle = \frac{1}{4}\langle A(t_1)A^*(t_2)\rangle + \frac{1}{4}\langle A^*(t_1)A(t_2)\rangle \tag{B2}$$

The correlation of the amplitudes can be expressed in terms of the Fourier transform of the green's function [Eq. (2.5)] as

$$\langle A(t_1)A^*(t_2)\rangle \cong \frac{N_e}{T_b}\int \frac{d(\Delta\omega)}{2\pi}|H(\Delta\omega)|^2 e^{i\Delta\omega(t_1-t_2)} \tag{B3}$$

Using Eq. (B3) in (B2), we find

$$\langle \varepsilon(t_1)\varepsilon(t_2)\rangle = \frac{N_e}{2T_b}\int_{-\infty}^{\infty} \frac{d(\Delta\omega)}{2\pi}|H(\Delta\omega)|^2 \cos[(\omega_s+\Delta\omega)(t_1-t_2)] \tag{B4}$$

In terms of the spectral density w(f) defined by Rice [18], this correlation of the electric fields can be expressed as

$$\langle \varepsilon(t_1)\varepsilon(t_2)\rangle = \int_0^{\infty} df\ w(f)\cos[2\pi f(t_1-t_2)] = \int_0^{\infty}\frac{d\omega}{2\pi} w(\frac{\omega}{2\pi})\cos[\omega(t_1-t_2)] \tag{B5}$$

Comparing Eqs. (B4) and (B5) we find

$$w\left(\frac{\omega_s+\Delta\omega}{2\pi}\right) = \frac{N_e}{2T_b}\left[|H(\Delta\omega)|^2 + |H(-\Delta\omega)|^2\right]. \tag{B6}$$

As noted after Eq. (2.11), $H(\Delta\omega)$ has a dependence on ω_s which we do not explicitly show.